Proceedings of the
Annual Stability Conference
Structural Stability Research Council
Toronto, Canada, March 25-28, 2014

Constrained Finite Strip Method Stability Analysis of Thin-walled Members with Arbitrary Cross-section

S. Ádány[1], B.W. Schafer[2]

Abstract

In this paper the generalization of the constrained finite strip method (*c*FSM) is discussed. *c*FSM is a special version of the semi-analytical finite strip method (FSM), where carefully defined constraints are applied which enforce the thin-walled member to deform in accordance with specific mechanics, e.g., to allow buckling only in flexural, lateral-torsional, or a distortional mode. In the original *c*FSM only open cross-section members are handled, here the method is extended to cover any flat-walled member, including those with closed cross-sections or cross-sections with open and closed parts. In the original *c*FSM only 4 deformation classes are defined, here the deformation field is decomposed into additional, mechanically meaningful, sub-fields, to which formal mechanical criteria are assigned. The method is implemented into the CUFSM software. The application and potential of the extended *c*FSM method is illustrated by numerical examples.

1. Introduction

Thin-walled members possess complicated stability behaviour. If subjected primarily to longitudinal stresses, three characteristic buckling classes are usually distinguished: global (G), distortional (D), and local-plate (L) buckling. Although in practical situations these modes rarely appear in isolation, typically some modal coupling is involved, the GDL classification has still been found useful for capacity prediction, and appears either implicitly or explicitly in current thin-walled design standards, e.g. NAS (2007), Eurocode 3 (2006). Capacity prediction requires the critical loads associated with the various buckling classes. Critical load calculation for thin-walled members is usually accomplished by some numerical methods, especially shell finite element method (FEM), generalized beam theory (GBT), see Silvestre et al (2011), or the finite strip method (FSM) which latter is in the focus of this paper.

FSM is based on the work of Cheung (1968), but popularized by Hancock (1978) who provided the organizing thrust of today's member design, which later evolved into the Direct Strength Method (DSM), see DSM (2006). Hancock introduced the notion of the signature curve, from

[1] Assoc. Professor, Budapest University of Technology and Economics, <sadany@epito.bme.hu>
[2] Professor, Johns Hopkins University, <schafer@jhu.edu>

which quasi-pure buckling modes and associated loads could be determined, at least for typical design. Accessibility of FSM was enhanced by the introduction of the open source software CUFSM, first for pin-ended, see CUFSM (2006), but later for other end restraints, see CUFSM (2012). Note, that in all these FSM implementations the primary loading is assumed to be longitudinal stresses, though recently FSM has also been applied to analyse shear buckling (Pham and Hancock, 2009) of thin-walled members.

Ádány and Schafer (2006a,b, 2008) proposed a special version of FSM, the constrained Finite Strip Method (*c*FSM). *c*FSM possesses the ability of modal decomposition as well as mode identification in a manner similar to GBT. In fact, *c*FSM and GBT have been found nearly coincident in their end results (Ádány et al, 2009), even though the roots of the two methods are distinctly different. Although *c*FSM can be considered as a theoretically interesting, and practically useful tool, it is not complete, having various limitations. The limitations are three-fold: (i) inherent limitations of FSM, (ii) limitations in the mechanical criteria used to separate the deformation classes, and (iii) originally only open cross-sections are covered. Whilst the first two sources of limitations are not addressed here, the current proposed generalization of *c*FSM completely removes the limitations with regard to cross-section topology, provided the cross-section can reasonably modelled as a set of flat thin-walled strips.

To be able to handle cross-sections with closed part(s), it is essential to carefully consider in-plane shear deformations, as shown in Ádány (2013), where the role of in-plane shear deformations are fully detailed. This leads to a decomposition of shear modes, which modes are the most important novelty of the here-introduced generalized *c*FSM. The new shear modes are required for the torsional behaviour of closed cross-sections, but also useful and practically meaningful for any cross-sections, and make it possible to reproduce global buckling modes similar to those of shear-deformable beam theories. Since the original derivations only applied to open cross-sections generalization of the cross-section and incorporation of the new shear modes requires new notations and formulation for *c*FSM, as presented here.

2. FSM and cFSM essentials

The finite strip method (FSM) is a shell-model-based discretization method. By utilizing longitudinal regularity, a common characteristic in thin-walled members, FSM requires a significantly smaller number of degrees of freedom (DOF) than the shell finite element method (FEM). Members are discretized into longitudinal strips as shown in Fig. 1. Note, in this paper (which focuses on primary modes only) only one strip per flat of the member is applied, as shown in Fig. 1. (Note, Fig. 1 illustrates the nodal displacements for the simplest longitudinal shape function as given in Eq. 4, with m=1.)

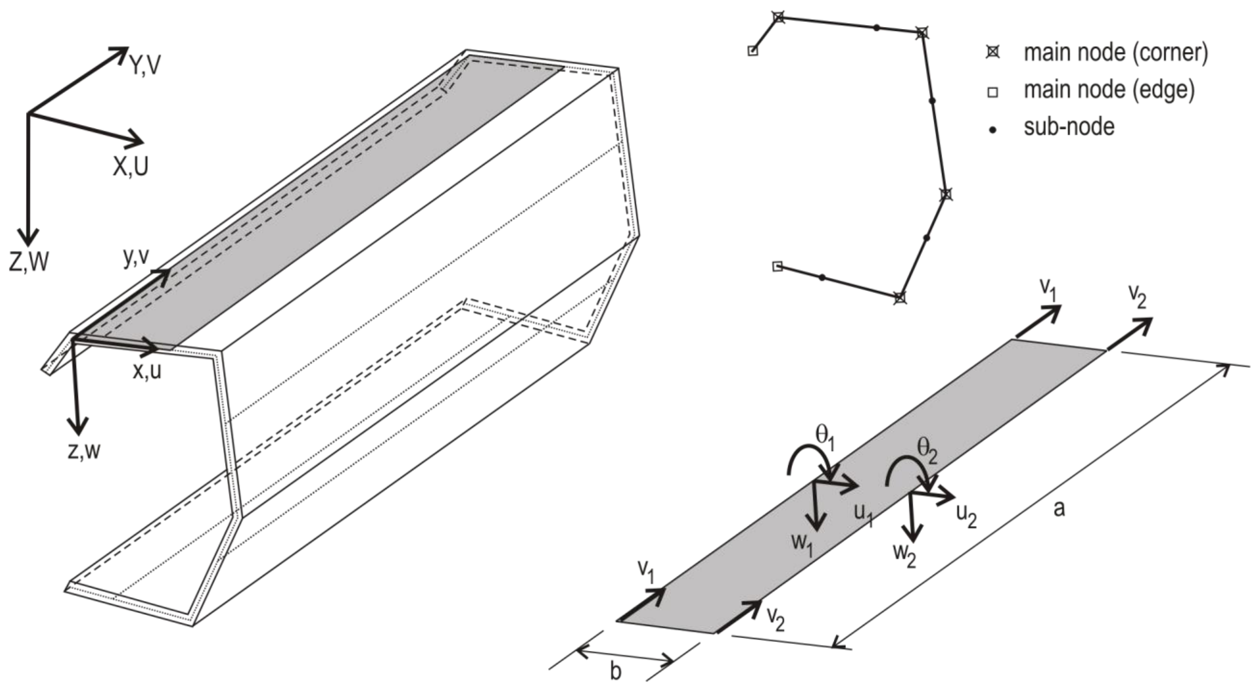

Figure 1: Finite strip discretization, strip DOF, and notation

Within a strip, local displacement fields *u*, *v*, and *w* are expressed as follows (Cheung, 1968):

$$u(x,y)=\sum_{m=1}^{q}\left[\left(1-\frac{x}{b}\right)\ \left(\frac{x}{b}\right)\right]\begin{bmatrix}u_{1[m]}\\ u_{2[m]}\end{bmatrix}Y_{[m]} \tag{1}$$

$$v(x,y)=\sum_{m=1}^{q}\left[\left(1-\frac{x}{b}\right)\ \left(\frac{x}{b}\right)\right]\begin{bmatrix}v_{1[m]}\\ v_{2[m]}\end{bmatrix}Y'_{[m]}\frac{a}{m\pi} \tag{2}$$

$$w(x,y)=\sum_{m=1}^{q}\left[\left(1-\frac{3x^2}{b^2}+\frac{2x^3}{b^3}\right)\ \left(-x+\frac{2x^2}{b}-\frac{x^3}{b^2}\right)\ \left(\frac{3x^2}{b^2}-\frac{2x^3}{b^3}\right)\ \left(\frac{x^2}{b}-\frac{x^3}{b^2}\right)\right]\begin{bmatrix}w_{1[m]}\\ \vartheta_{1[m]}\\ w_{2[m]}\\ \vartheta_{2[m]}\end{bmatrix}Y_{[m]} \tag{3}$$

where *a* is the member length, and *b* is the strip width. For the simplest pin-pin end restraints the longitudinal shape functions are as follows:

$$Y_{[m]}=\sin\frac{m\pi y}{a}\quad\text{and}\quad Y'_{[m]}\frac{a}{m\pi}=\cos\frac{m\pi y}{a} \tag{4}$$

In this case the solution can be found for any *m* term independently of the other *m* terms, i.e., the *m* terms are uncoupled. For other end restraints (e.g. clamped-clamped) other functions are necessary, (Li and Schafer, 2010), and the *m* terms are coupled.

The local elastic and geometric stiffness matrices can be constructed by following conventional FEM steps, by considering the 2D generalized Hooke's law (for the constitutive matrix) and by considering the second-order strain terms (for the geometric matrix). The stiffness matrices can be determined analytically. The size of the local strip stiffness matrices for a specific *m* term is 8 by 8, while for the series solution: (8×*q*) by (8×*q*), where *q* is the number of considered terms in the longitudinal shape functions.

From the local stiffness matrices the member's (global) stiffness matrices (elastic and geometric, $\mathbf{K_e}$ and $\mathbf{K_g}$) can be compiled as in FEM, by transformation to global coordinates and assembly. The size of the global matrices is (4×*n*×*q*) by (4×*n*×*q*), where *n* is the number of nodal lines.
For a given distribution of edge tractions on a member the geometric stiffness matrix scales linearly, resulting in the classic eigen-buckling problem, namely:

$$\mathbf{K_e \Phi} - \mathbf{\Lambda K_g \Phi} = \mathbf{0} \tag{5}$$

with

$$\mathbf{\Lambda} = diag\lfloor \lambda_1 \quad \lambda_2 \quad \dots \quad \lambda_{4nq} \rfloor \text{ and } \mathbf{\Phi} = \lfloor \varphi_1 \quad \varphi_2 \quad \dots \quad \varphi_{4nq} \rfloor \tag{6}$$

where λ_i is the critical load multiplier and $\boldsymbol{\varphi}_i$ is the mode shape vector (i = 1..4nq).

The constrained FSM (*c*FSM) is an extension to FSM that uses mechanical assumptions to enforce or classify deformations to be consistent with a desired set of criteria. The method is presented in Ádány and Schafer (2006a,b, 2008), and implemented in CUFSM. The *c*FSM constraints are mechanically defined, as in Table 1, and are utilized to formally categorize deformations into global (G), distortional (D), local (L), and other (i.e., shear and transverse extension, S+T) deformations. Specifically, any FSM displacement field **d** (e.g. an eigen-buckling mode $\boldsymbol{\varphi}$ is an important special case) may be constrained to any deformation space (or mode space) M via:

$$\mathbf{d} = \mathbf{R_M d_M} \tag{7}$$

where $\mathbf{R_M}$ is a constraint matrix, the derivation of which can be found in Ádány and Schafer (2006a,b, 2008) for open cross-sections, and M might be G, D, L, S and/or T.
Modal decomposition of the eigen-buckling solution is completed by introducing the desired constraint matrix $\mathbf{R_M}$, the columns of which can be interpreted as base vectors for the given M space. Applying $\mathbf{R_M}$ for the intended space (M = G, D, L, S, and/or T) Eq. 5 becomes:

$$\mathbf{R_M}^{\mathrm{T}}\mathbf{K_e R_M \Phi_M} - \mathbf{\Lambda_M R_M}^{\mathrm{T}}\mathbf{K_g R_M \Phi_M} = \mathbf{0} \tag{8}$$

$$\mathbf{K_{eM} \Phi_M} - \mathbf{\Lambda_M K_{gM} \Phi_M} = \mathbf{0} \tag{9}$$

where $\mathbf{K_{eM}}$ and $\mathbf{K_{gM}}$ are reduced-size elastic and geometric stiffness matrices for the eigen-buckling solution constrained to space M.

Table 1: Mechanical criteria for mode classes in original *c*FSM

	G	D	L	S/T
$\varepsilon_x = \partial u/\partial x = 0$ & $\gamma_{xy} = \partial u/\partial y + \partial v/\partial x = 0$	Y	Y	Y	N
$v \neq 0$ & transverse equilibrium	Y	Y	N	-
$\kappa_x = \partial^2 w/\partial x^2 = 0$	Y	N	-	-

Modal identification, i.e. categorization of a general deformation into the M spaces, is also possible, due to the fact that G+D+L+S+T spans the entire FSM space. As such, the $\mathbf{R_{GDLST}}$ constraint matrix represents an alternative basis for the FSM space, in which deformations are categorized. This basis transformation of displacement vector **d** may be expressed as:

$$\mathbf{d} = \begin{bmatrix} \mathbf{R_G} & \mathbf{R_D} & \mathbf{R_L} & \mathbf{R_{ST}} \end{bmatrix} \mathbf{c} \tag{10}$$

where **c** now provides the deformations within each class: $\mathbf{c_G}$, $\mathbf{c_D}$, $\mathbf{c_L}$, $\mathbf{c_{ST}}$. The values of **c** are dependent on the normalization of the base vectors within **R**. A full discussion of the normalization selection for **R** is provided in (Li et al, 2011). Once **c** is determined, p_i participation of an individual mode or p_M participation of a deformation space M can also be determined as follows:

$$p_i = \|\mathbf{c}_i\| / \|\mathbf{c}\| \quad \text{or} \quad p_M = \|\mathbf{c_M}\| / \|\mathbf{c}\| \tag{11}$$

3. Generalized *c*FSM

3.1 Basics for generalized cFSM

Generalized *c*FSM, presented here for the first time, extends *c*FSM (and modal identification and decomposition) to closed cross-sections and cross-sections with both open and closed portions. To meaningfully achieve this goal a number of changes are implemented. An important necessity for generalized *c*FSM is the application of (in-plane) shear modes as proposed and discussed in (Ádány, 2013). Note, here the phrase shear mode does not imply shear buckling, as in (Pham and Hancock, 2009), since the assumed loading is longitudinal tension and/or compression stress (similar to other FSM/ *c*FSM or GBT papers).

Along with the introduction of new shear modes, the spaces are further subdivided into smaller sub-spaces. First, L, S and T mode spaces are separated into primary and secondary mode spaces. Primary modes are those deformations which are completely defined by the degrees of freedom (DOF) associated with the main nodes only, i.e., those nodes at the junction or end of the flat plates comprising the section. Secondary modes are defined by the DOF of the sub-nodes, i.e. those nodes within a flat plate discretized into multiple strips. It is to note that G and D modes are – by definition – primary modes, i.e., determined solely by main node displacements.

Here a short description is given for all the introduced spaces and sub-spaces as follows.

- G is the *global* space, which involves rigid-body transverse displacements and associated warping displacements so that the no transverse extension and no (in-plane) shear criteria are satisfied. It is subdivided into sub-spaces as follows:
  - G_A is the *axial* space, which involves uniform warping displacement only.
  - G_B is *global bending* space, the sub-space of G space consisted of two bending modes. G_B involves rigid-body transverse displacements of the cross-section, and associated with warping, too, with linear warping distribution over the cross-section.
  - G_T is *global torsion* space, that involves the rigid-body torsion of the cross-section, and since it is part of the G space, it is shear free (therefore typically associated with warping displacements, too). G_T exists only if the cross-section is open, since if the cross-section is closed or has closed part(s), shear-free torsion is physically impossible.
- D is *distortional* space, where the no transverse extension and no (in-plane) shear criteria are satisfied, but the cross-section is distorted and warping is non-zero (but piece-wise linear).
- L is the *local* space, which involves deformations similar to local plate-buckling. It is subdivided into sub-spaces as follows:
  - L_P is *primary local* space, which involves deformations generated as if no sub-nodes would exist.
  - L_S is *secondary local* space, characterized by zero displacements at main nodes and non-zero displacements at sub-nodes.
- S is the *shear* space, characterized non-zero in-plane shear strain. Two kinds of shear space can and are useful to distinguish, as follows.
  - S_w is *warping-only shear* space, characterized by non-zero in-plane shear strain and by linear (i.e., linear between two nodes) warping displacements and zero transverse displacements. Within this space the following sub-spaces are defined.
    - S_{Bw} is *warping-only shear bending* space, characterized by warping displacements identical to those of G_B, therefore S_{Bw} is primary mode space.
    - S_{Tw} is *warping-only shear torsion* space, characterized by warping displacements identical to those of G_T. If G_T does not exist, S_{Tw} does not exist, neither. S_{Tw} is primary mode space.
    - S_{Dw} is *warping-only shear distortional* space, characterized by warping displacements identical to those of D, therefore S_{Dw} is primary mode space.
    - S_{Cw} is *warping-only other shear* space, sub-space of S_w, which is not part of any of S_{Bw}, S_{Tw}, and S_{Dw}, but characterized by linear warping displacements between two main nodes, therefore S_{Cw} is primary mode space.

        - S_S is *secondary (warping-only) shear* space, sub-space of S_w, but characterized by non-linear warping displacements between two main nodes, therefore S_S is a secondary mode space.
    - S_t is *transverse-only shear* space, characterized by non-zero in-plane shear strain and non-zero transverse displacements and zero warping displacements. S_t is primary mode space, and can be sub-divided into the following sub-spaces:
        - S_{Bt} is *transverse-only shear bending* space, characterized by rigid-body cross-sectional transverse translational displacements identical to those of G_B.
        - S_{Tt} is *transverse-only shear torsion* space, characterized by rigid-body cross-sectional torsional displacements, identical to those of G_T. If G_T does not exist, S_{Tt} does still exist, since rigid-body torsional displacements for the cross-section can always be applied.
        - S_{Dt} is *transverse-only shear distortional* space, characterized by transverse displacements identical to those of D.
        - S_{Ct} is *transverse-only other shear* space, sub-space of S_t, which is not part of any of S_{Bt}, S_{Tt}, and S_{Dt}.
- T is *transverse extension* space, characterized by zero warping and non-zero transverse extension/shortening (in the mid-planes). It can be subdivided into sub-spaces as follows:
    - T_P is *primary transverse extension* space, generated as if no sub-nodes would exist, which is resulted in constant transverse strain in between two main nodes.
    - T_S is *secondary transverse extension* space, characterized by zero displacements at main nodes and non-zero displacements at sub-nodes, which is resulted in non-constant transverse strain in between two main nodes.

3.2 Construction of the spaces

For the construction of the base system (R_M) for any deformation space, three kinds of criteria are employed: null, independence and orthogonality.

- For any space or sub-space some strain components are set to zero, these define the *null criteria*. In some cases it is also necessary to examine whether transverse equilibrium of the cross-section is satisfied or not. Since transverse equilibrium means that unbalanced nodal forces/moments are zero, transverse equilibrium is also treated as a *null criterion*, which, again, can easily be enforced.
- Furthermore, the spaces, that is G, D, L, S and T must be linearly independent, leading to the *independence criteria*.
- Finally, the sub-spaces within a space must be orthogonal (in certain sense) leading to the *orthogonality criteria*. For example, G_A and G_B and G_T, all being part of space G, must be orthogonal to each other.

Table 2 summarizes the null criteria. Three in-plane strains and three out-of-plane curvatures are considered as follows:

$$\varepsilon_x = \partial u / \partial x \quad \varepsilon_y = \partial v / \partial y \quad \gamma_{xy} = \partial u / \partial y + \partial v / \partial x \tag{12}$$

$$\kappa_x = \partial^2 w / \partial x^2 \quad \kappa_y = \partial^2 w / \partial y^2 \quad \kappa_{xy} = \partial^2 w / \partial x \partial y \tag{13}$$

where all the u, v and w functions are interpreted at the middle surface of the plates (i.e., at $z = 0$).

Table 2 indicates whether the given criterion is satisfied or not (Y or N, respectively) in the given space or sub-space. Here are a few important comments as follows.

It is to observe that between the various warping-only S modes there is no mechanical difference, they are separated on the basis of warping distribution, by using the warping distributions of G and D modes.

Although Table 2 is virtually different from Table 1, there is no conflict between the two tables: the new mode definition table does not modify the original mode definitions, it only gives more details. In fact, those cells are highlighted in Table 2 which contain the same information as Table 1. Note, the distributions of v and ε_y along any cross-section line are identical, therefore $v \neq 0$ and $\varepsilon_y = 0$ are opposing criteria.

Table 2: Null criteria for mode classes in generalized *c*FSM

	G			D	L		S									T	
	G_A	G_B	G_T		L_P	L_S	S_{Bt}	S_{Tt}	S_{Dt}	S_{Ct}	S_{Bw}	S_{Tw}	S_{Dw}	S_{Cw}	S_S	T_P	T_S
$\varepsilon_x=0$	Y			Y	Y		Y									N	
$\gamma_{xy}=0$	Y			Y	Y		N									N	
eq.	Y			Y	N		Y	Y	Y	N	Y	Y	Y	Y	Y	N	
$\varepsilon_y=0$	N			N	Y		Y	Y	Y	Y	N	N	N	N	N	Y	
$\kappa_x=0$	Y			N	N		Y	Y	N	N	Y	Y	Y	Y	Y	N	Y
$\kappa_{xy}=0$	Y	Y	N	N	N	N	Y	N	N	N	Y	Y	Y	Y	Y	N	Y
$\kappa_y=0$	Y	N	N	N	N	N	N	N	N	N	Y	Y	Y	Y	Y	N	Y

For G and S modes there is a special issue, discussed by Ádány (2013). G_B and S_{Bw} vectors have the same warping displacements, while G_B and S_{Bt} have the same transverse displacement. (Note the scaling can be different, but any mode vector can arbitrarily be scaled.) Thus, summing S_{Bw} and S_{Bt} yields G_B, and the three spaces are linearly dependent. Only two of the three spaces can and must be selected. Exactly the same is true for G_D, S_{Dw} and S_{Dt}; therefore, only two of these three spaces can and must be selected.

As far as G and S torsion modes are concerned, for open cross-sections all G_T, S_{Tw} and S_{Tt} are existing and linearly dependent as bending or distortional modes. If the cross-section is closed or has closed part(s), G_T does not exist, consequently S_{Tw} does not exist. S_{Tt} still (and always) exists, and does not overlap.

From a practical aspect it is deemed beneficial to have shear-free modes (i.e., G modes) if they exist, to which either warping-only or transverse-only shear modes can be selected, based on the user's choice, as illustrated in Fig. 2.

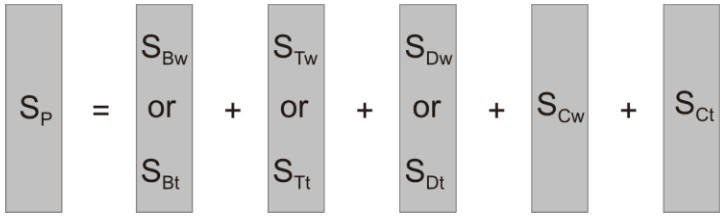

Figure 2: Compilation of the base system for primary shear mode

Detailed derivations for the base vectors would be too long to present here (but will be presented in future publications). Nevertheless, the various criteria can be expressed by matrices, thus, the various criteria can be enforced by matrix equations. The process is already implemented into a special version of CUFSM software.

A final comment is that the above-summarized process of mode construction leads to unambiguous and distinct sub-spaces for most of the cross-sections. However, overlapping of sub-spaces happens if the cross-section is too simple, namely, if it has zero or one main node. The problem is not discussed here, but it is to mention that it can easily be handled.

3.3 Illustration of the spaces

Primary modes are those deformations that are associated with minimal cross-section discretization, i.e. nodal lines located at folds and ends only. When primary modes are constructed, sub-nodes are disregarded. Fig. 3 shows all the primary modes of a two-cell cross-section member.

The simplest way to construct base vectors for secondary modes is to apply 1's and 0's at the sub-nodes for the relevant degrees of freedom, while keeping all main node DOF fixed at zero. For a single plate with 4 sub-nodes (5 strips) the resulting base systems are illustrated in Figs. 4-6. (Note, S_S base vectors for a whole cros-section are presented in the Appendix.)

3.4 Orthogonalization within a mode space

The construction of the deformation spaces determines the deformation spaces, defined by their base vectors (functions). However, various systems of base vectors are possible (unless the space is one-dimensional such as A, or G_T), of which some might be practically more useful than another. From a practical aspect, orthogonalized base systems are of special importance, since orthogonal base vectors may be useful for reducing the size of the problem to be solved, or isolating and examining a particular behavior in detail. Moreover, orthogonality of the base vectors is desired when mode identification is performed.

Two basic interpretations with respect to orthogonality are considered: (i) orthogonality in cross-section sense, and (ii) orthogonality in member sense. Orthogonality in the member sense is included in CUFSM and detailed in (Li et al, 2011) and not discussed here further. Orthogonality in the cross-section sense has the important feature that the base vectors are intended to be determined independently of the longitudinal shape functions, i.e. independent of member length, end restraints, and loading. This kind of orthogonality is discussed here as follows.

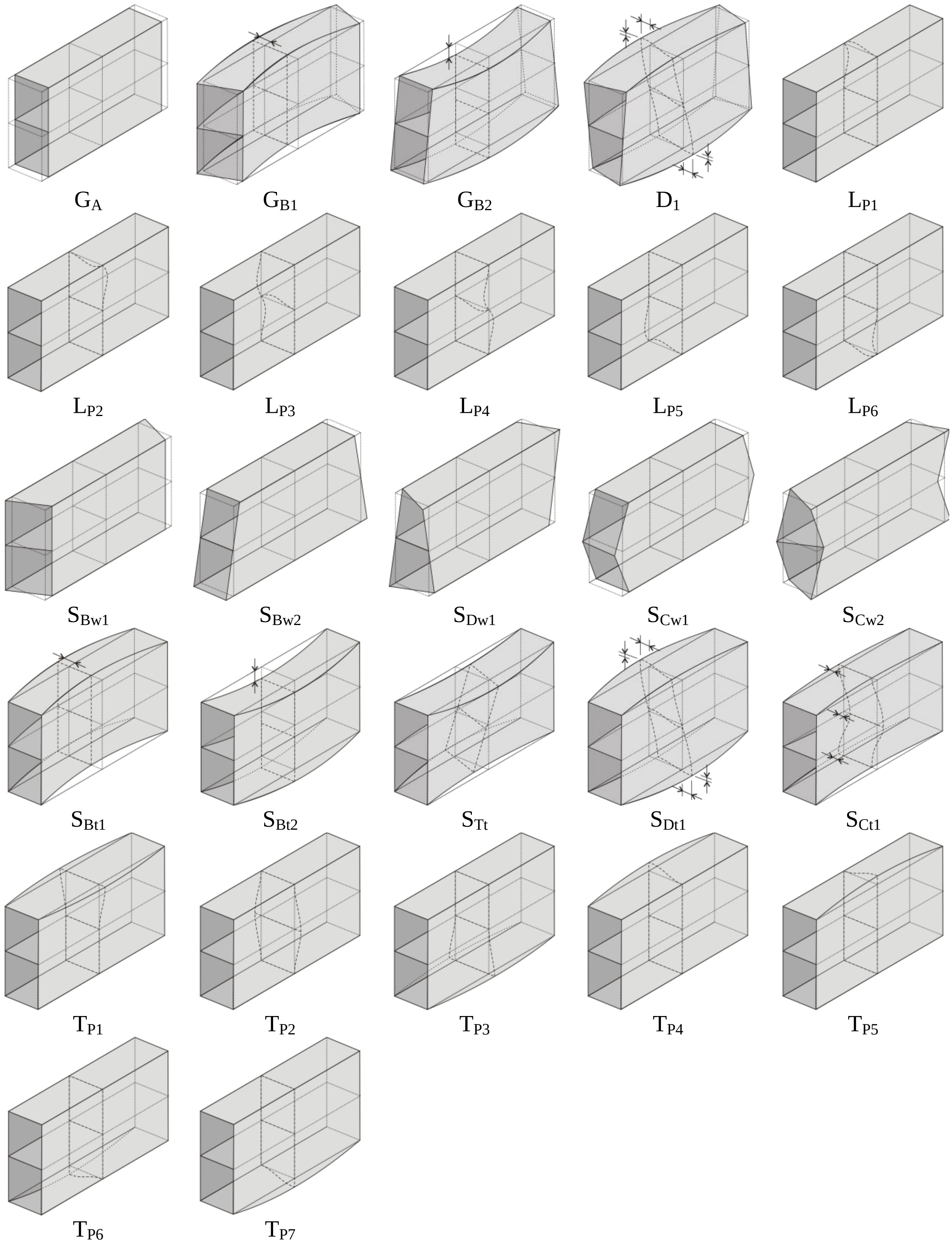

Figure 3: Primary modes of a two-cell cross-section

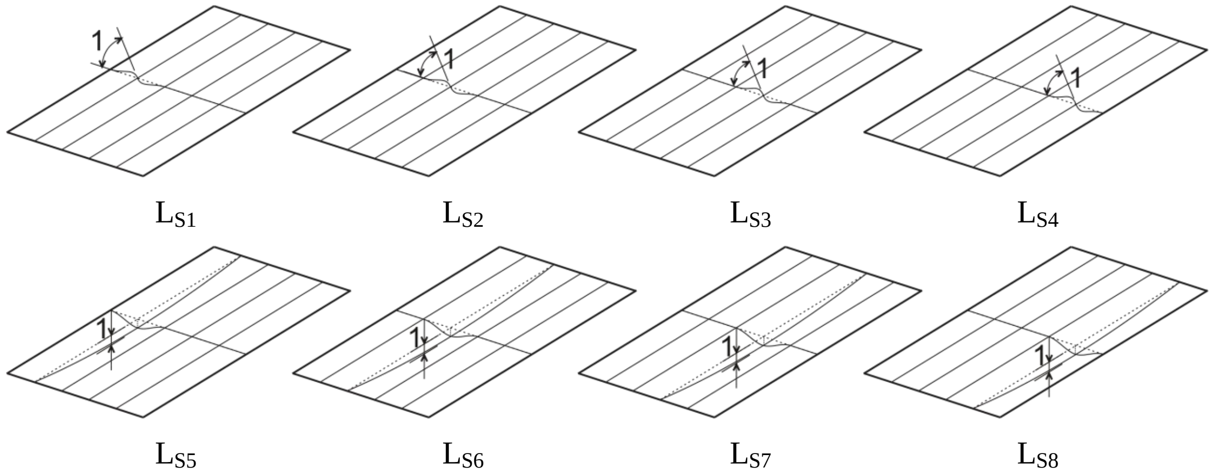

Figure 4: Base system for secondary local space of a single plate

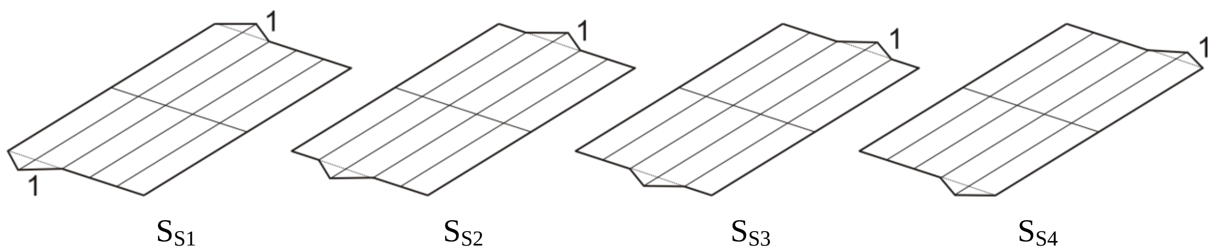

Figure 5: Base system for secondary shear space of a single plate

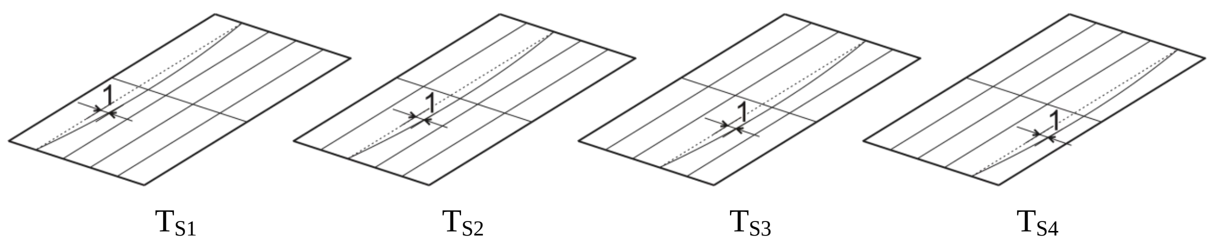

Figure 6: Base system for secondary transverse extension space of a single plate

Cross-section orthogonal base vectors (functions) imply: (i) some displacement functions (or their derivatives) are orthogonal to each other, (ii) the orthogonality is satisfied by base vectors within the same deformation space, and (iii) the orthogonality is interpreted within cross-sections (rather than in the member). Mathematically, this implies:

$$\int f_r f_s ds = 0 \text{ if } r \neq s \text{ and } \int f_r f_s ds \neq 0 \text{ if } r = s \tag{14}$$

where f is a displacement function (or its appropriate derivative), which can be determined from a displacement vector. Since orthogonality is for the cross-section (rather than for the whole member), f must be selected so that it would be characteristic for the cross-section. Similar orthogonality condition has already been applied during the construction of the deformation spaces. The most well-known of such orthogonality condition is the orthogonality of warping functions within the G_D space. These functions are characteristic for G and D spaces, thus, can readily be used to create orthogonal mode vectors. For other spaces other functions might be advantageous. For the potentially multi-dimensional primary spaces the proposed functions are summarized in Table 3.

Table 3: Orthogonality criteria for the multidimensional spaces

	primary						secondary		
mode space	G_B	D	L_P	S_{Cw}	S_{Ct}	T_P	L_S	S_S	T_S
displ. function for orthogonality	ε_y	κ_x	κ_x	γ_{xy}	γ_{xy}	ε_x	κ_x	γ_{xy}	ε_x

It is to note that S_B and S_D spaces are (or can be) multi-dimensional, too. However, these spaces are tied to G_B and D, therefore, if G_B and D are orthogonalized, S_B and S_D are automatically orthogonalized in the same way. Orthogonal base system is shown in the Appendix.

For mode identification the (orthogonal) base vectors must be scaled. For scaling a simple straightforward way is selected: set the maximum value of a characteristic displacement component to 1 in a given base vector. The characteristic displacement component can be the local *w* for G_B, G_T, D, L (including both primary and secondary L) and S_t modes, the local *v* for G_A and warping-only S_w modes (including secondary shear modes), and the local *u* for T modes (both primary and secondary).

4. Numerical examples

In this Section a numerical examples are provided to illustrate the novel features of the new, generalized *c*FSM. A beam with a hollow-flange U cross-section is discussed. The cross-section and its dimensions are shown in Fig. 7.

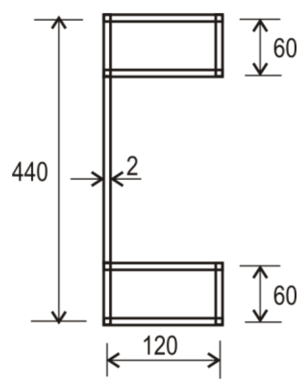

Figure 7: Geometry of the analyzed hollow-flange U-beam (dimensions in mm)

In applying *c*FSM, first the FSM deformation space must be decomposed into the G, D, L, S and T spaces and their sub-spaces. While (number and shape of) primary modes are independent of the applied discretization, (number and shape of) secondary modes are strongly influenced by the sub-nodes. For a rough discretization, with having three sub-nodes in the web only, deformation modes are presented in the Appendix, where both (possible) non-orthogonal and orthogonal base vectors are shown. It is to mention that the base vectors are independent of the loading, material properties, member length or end restraints.

For the given beam member with the considered cross-section critical stresses are calculated employing several options. Pin-pin end restraints are applied. The considered material constants are as follows: E = 210 MPa, G = 105 MPa, ν = 0. It is to note that the Poisson's ratio is assumed to be zero for no other reason than to avoid the artificial stiffening effect of restrained (mid-plane) transverse extension which takes place in G and D modes for non-zero Poisson's ratios, as discussed in detail in (Ádány et al, 2009). It is to emphasize that during the calculations a fine enough discretization is applied (i.e., finer than the one illustrated by the figures of the Appendix).

In Table 4, first, the effect and importance of shear deformations is illustrated. "Pure" global buckling, that is lateral-torsional buckling is calculated in 4 options, with neglecting and considering shear deformations. As it is clear from the numerical results, LTB is practically impossible without in-plane shear, since the no-shear criterion completely eliminates the twist of the cross-sections (see the G option). As soon as some shear is allowed, the buckled shape will involve lateral translation and torsion, therefore, can reasonably be categorized as lateral-torsional buckling. The value of the calculated critical stress depends on the considered shear modes. Comparison of $G+S_P$ and $G+S_P+S_S$ options suggests that the S_S secondary shear modes have small effect and limited to (fairly) short members only. Comparison of $G+S_T$ and $G+S_P$ options, however, highlights that consideration of all the S_P primary shear modes leads to significant critical stress reduction compared to the case when the S_T shear torsion mode is considered only.

Table 4: Critical stresses for lateral-torsional buckling of the hollow-flange U-beam

length (mm)	50	100	200	500	1000	2000	5000	10000
G	265582	265582	265582	265582	265582	265582	265582	265582
$G+S_T$	261175	215409	113932	45886.8	22962.3	11483.5	4593.65	2296.84
$G+S_P$	69508.9	61643.4	44945.9	18591.9	7454.44	3119.97	1149.61	566.859
$G+S_P+S_S$	67108.1	58620.7	42474.8	17811.1	7318.02	3103.16	1148.58	566.731

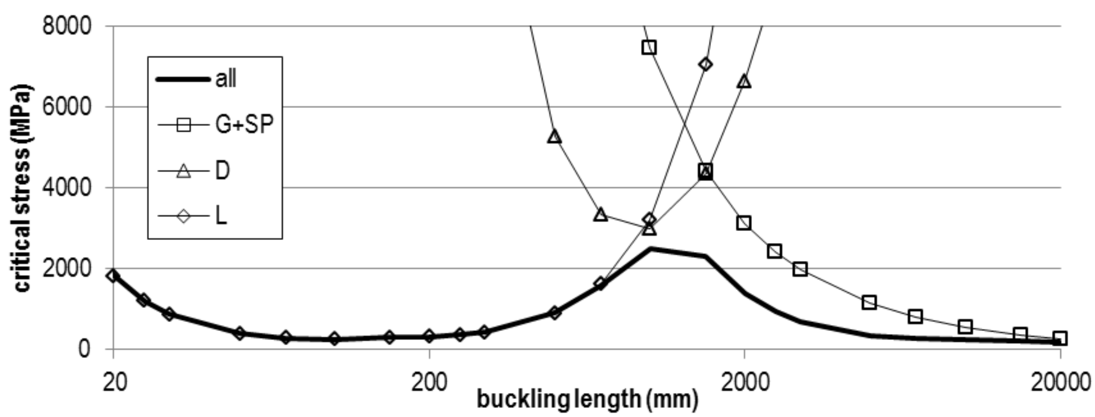

Figure 8: All-mode and quasi-pure-mode curves for the analyzed hollow-flange U-beam

Fig. 8 compares the all-mode solution (i.e., classic FSM solution), and pure "global", distortional, and local buckling solutions. (For the "pure" global mode, the G+S_P solution is selected.) Note, such comparison was not possible with the original *c*FSM method, but can be done without any problem by using the generalized *c*FSM presented here.

The modal identification of the all-mode curve (i.e., so-called signature curve) is shown in Fig 9, where G, D, L, S and T participations are given in percentages as a function of length. Selected buckled mode shapes and modal participations are provided in Fig 10. Here are some comments as follows.

- Two local buckled shapes exist with nearly identical minimal critical stresses: for short buckling lengths local-plate buckling of the most compressed flange governs, while for slightly longer buckling lengths local-plate buckling of the compressed part of the web governs.
- Though participation of D is never more than 50%, it has non-negligible participation for any length larger than approx. 1000 mm. Moreover, D's small participation significantly decreases the critical stress at large buckling lengths.
- For shorter lengths, when the buckling mode is (nearly) pure local, the buckled shape is superposed from multiple local individual modes, including practically all the primary local modes and a few secondary local modes. For longer lengths the buckled shape consists of only a few modes. For example, at 2500 mm, only two individual modes have significant participation: G_{B1} and D_1. Similarly, at 15000 mm, only four individual modes have significant participation: G_{B1} and D_1, and S_T and S_{D1}.
- It is found that transverse extension modes have negligible importance in the analysed case.

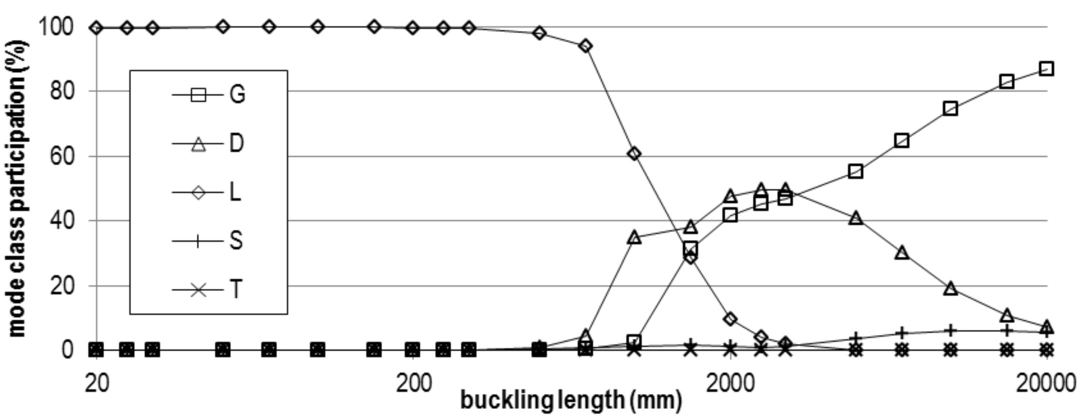

Figure 9: Mode participations in all-mode curve for the hollow-flange U-beam

buckled shape	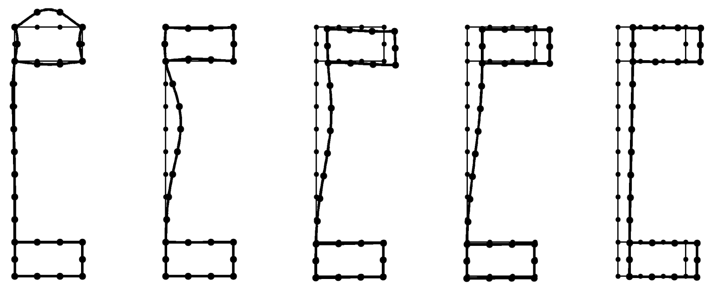				
length (mm)	100	300	1500	2500	15000
G %	0.0	0.0	31.4	45.2	82.8
D %	0.1	0.2	38.2	49.8	11.0
L %	99.7	99.4	28.7	4.1	0.0
S %	0.2	0.4	1.6	1.0	6.2
T %	0.0	0.0	0.0	0.0	0.0

Figure 10: Buckled shape samples, all-mode, hollow-flange U-beam

5. Concluding remarks

In this paper the generalization of the constrained Finite Strip Method (*c*FSM) is introduced. The most important novel features are summarized as follows.

While the original *c*FSM proposal handles open cross-section members only, the generalized method covers virtually any flat-walled member, including those with closed cross-sections or cross-sections with open and closed parts.

Exclusion of closed cross-sections from original *c*FSM was (mostly) due to the superficial handling of in-plane shear deformations. In-plane shear deformations are carefully considered and applied by the generalized method. In other words, the generalized *c*FSM provides a theoretically and practically meaningful decomposition for the in-plane shear deformations.

In the original *c*FSM only 4 deformation classes are defined (i.e., G, D, L and S/T). In the generalized *c*FSM the deformation field is decomposed into smaller sub-fields. Introduction of sub-fields is, first of all, necessary for the shear mode decomposition, as well it provides with a fine control on the considered deformation field (e.g., whether warping is linear or non-linear in between two main nodes). Formal mechanical criteria are given for all the mode spaces and sub-spaces.

The implementation of the mechanical criteria is generalized. In the new *c*FSM proposal no preliminary assumption is necessary regarding the cross-section topology. Moreover, no cross-section properties are necessary or used. Thus, though beam-model-based results can be reproduced, the here presented generalized *c*FSM is completely independent of beam models.

It is believed that the introduction of the generalized *c*FSM, as briefly presented here, is an important step toward an even more generalized decomposition method based on shell finite elements.

Acknowledgments
The presented work was conducted with the financial support of The Hungarian American Enterprise Scholarship Fund and the OTKA K108912 project of the Hungarian Scientific Research Fund.

References

NAS (2007). North American specification for the design of cold-formed steel structural members. 2007 ed. Washington DC, USA, American Iron and Steel Institute, 2007.

Eurocode 3 (2006). EN 1993-1-3, General rules, Supplementary rules for cold-formed members and sheeting, October 23, 2006.

Silvestre N., Camotim D., Silva N.F. (2011). "Generalized Beam Theory revisited: from the kinematical assumptions to the deformation mode determination", *Int. Journal of Structural Stability and Dynamics*, 11(5), Oct 2011, pp. 969-997.

Cheung Y.K. (1968). Finite strip method in the analysis of elastic paltes with two opposite ends simply supported, *Proc Inst Civ Eng*, 40, 1-7, 1968.

Hancock, G.J. (1978). „Local, Distortional, and lateral buckling of I-beams*"*, ASCE *Journal of structural engineering*, 104(11), pp. 1787-1798, 1978.

DSM (2006). Direct strength method design guide. American Iron and Steel Institute. Washington, DC, USA, 2006.

CUFSM (2006). Elastic Buckling Analysis of Thin-Walled Members by Finite Strip Analysis. CUFSM v3.12, http://www.ce.jhu.edu/bschafer/cufsm

CUFSM (2012). Elastic Buckling Analysis of Thin-Walled Members by Finite Strip Analysis. CUFSM v4.05, 2012. http://www.ce.jhu.edu/bschafer/cufsm

Pham, C.H., Hancock, G.J. (2009). "Shear buckling of thin-walled channel sections", *Journal of Constructional Steel Research*, vol. 65, no. 3, 2009, pp. 578-585.

Ádány, S., Schafer, B.W. (2006a) "Buckling mode decomposition of single-branched open cross-section members via Finite Strip Method: derivation", *Thin-Walled Structures* **44**(5), pp. 563-584, 2006.

Ádány, S., Schafer, B.W. (2006b). "Buckling mode decomposition of single-branched open cross-section members via Finite Strip Method: application and examples", *Thin-Walled Structures*, **44**(5), pp. 585-600, 2006.

Ádány, S., Schafer, B.W. (2008). "A full modal decomposition of thin-walled, single-branched open cross-section members via the constrained finite strip method", *Journal of Constructional Steel Research*, 64 (1), pp. 12-29, 2008.

Li, Z., Hanna, M.T., Ádány, S., Schafer, B.W. (2011). "Impact of basis, orthogonalization, and normalization on the constrained Finite Strip Method for stability solutions of open thin-walled members", *Thin-Walled Structures*, vol. 49, no. 9, pp. 1108-1122, 2011.

Ádány, S., Silvestre, N., Schafer, B.W., Camotim, D. (2009). "GBT and cFSM: two modal approaches to the buckling analysis of unbranched thin-walled members", *Int. Journal Advanced Steel Construction*, Vol. 5, No. 2, pp. 195-223, 2009.

Ádány S. (2013). "Decomposition of in-plane shear in thin-walled members", *Thin-Walled Structures*, Vol 73, pp 27-38.

Li, Z., Schafer, B.W. (2010). "Buckling analysis of cold-formed steel members with general boundary conditions using CUFSM: Conventional and constrained finite strip methods", *Proceedings* of the 20th International Specialty Conference on Cold-Formed Steel Structures - Recent Research and Developments in Cold-Formed Steel Design and Construction, p. 17., 2010.

Appendix: The full set of modes for a hollow-flange U-beam

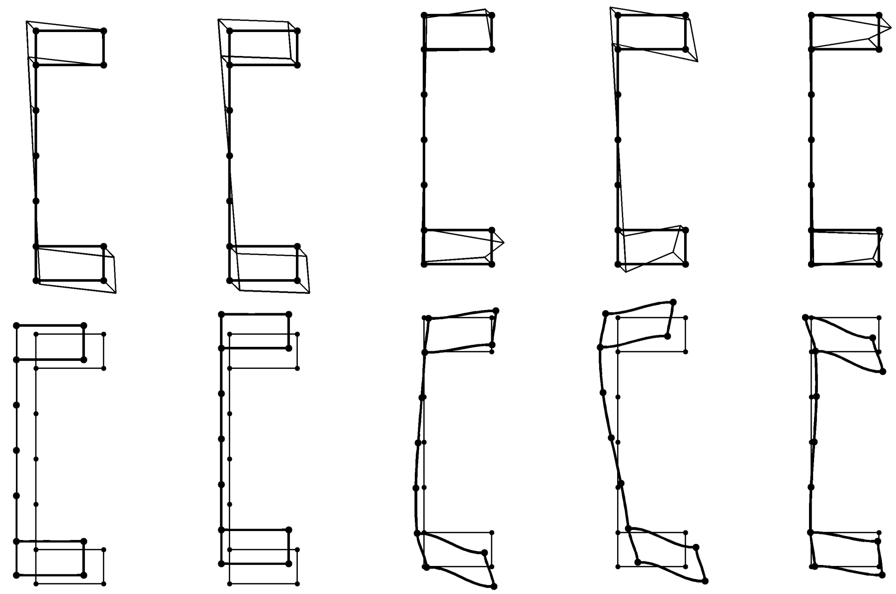

G_{B1} G_{B2} D_1 D_2 D_3

Figure A1: Native base system for the G_B and D spaces

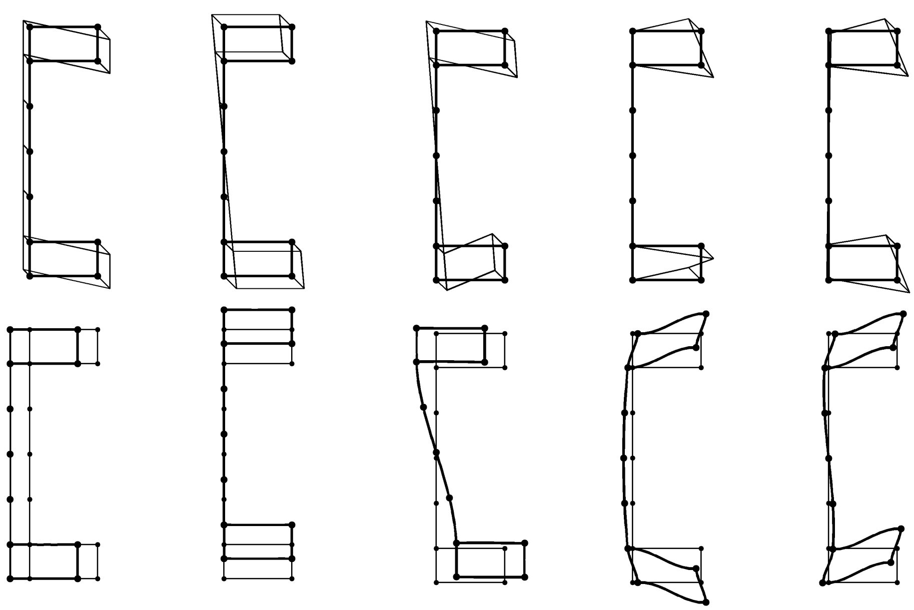

G_{B1} G_{B2} D_1 D_2 D_3

Figure A2: Cross-section orthogonal base system for the G_B and D spaces

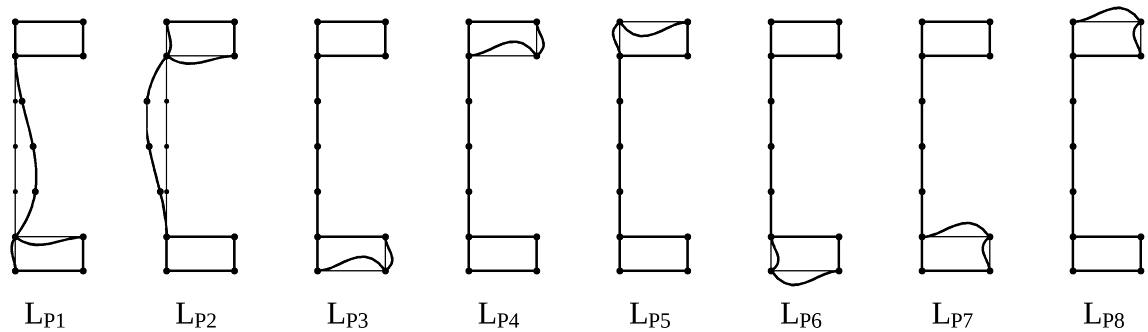

Figure A3: Native base system for the L_P space

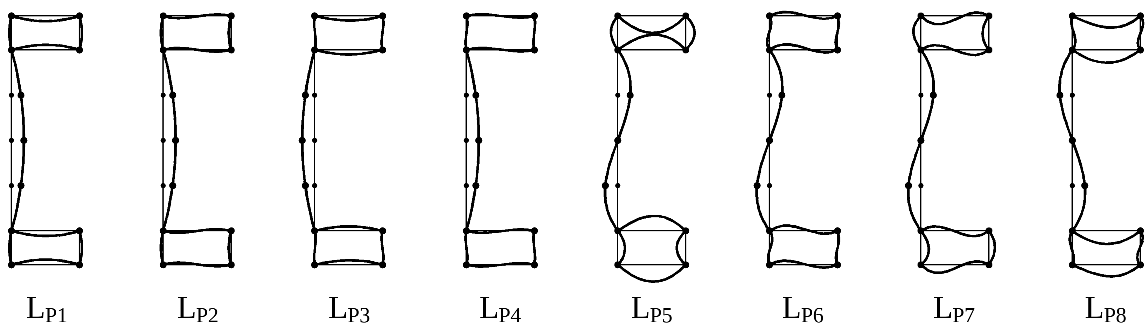

Figure A4: Cross-section orthogonal base system for the L_P space

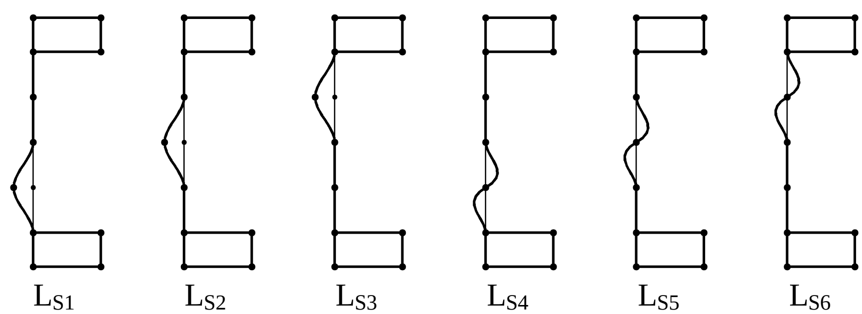

Figure A5: Native base system for the L_S space

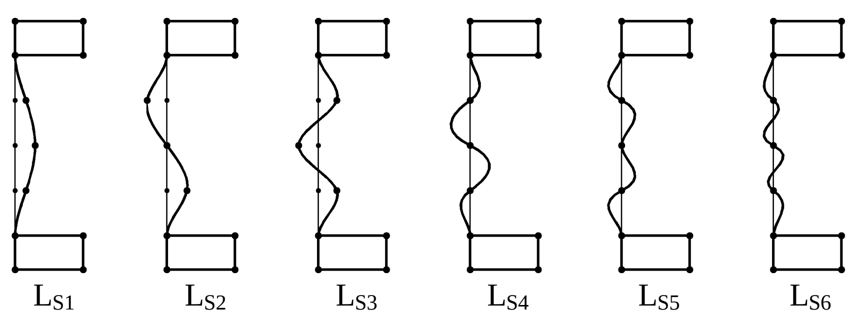

Figure A6: Cross-section orthogonal base system for the L_S space

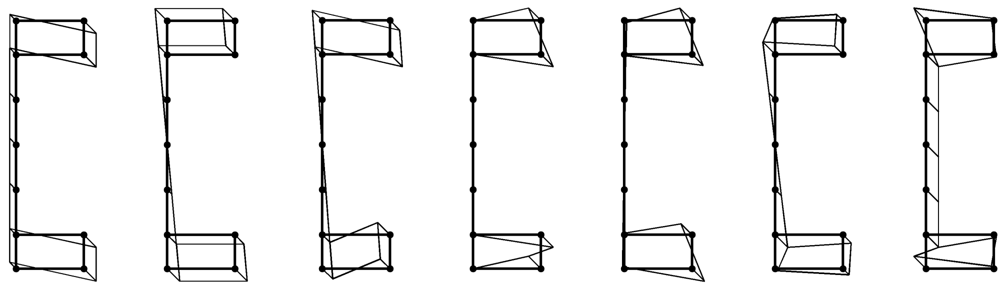

S_{Bw1} S_{Bw2} S_{Dw1} S_{Dw2} S_{Dw3} S_{Cw1} S_{Cw2}

Figure A7: Cross-section orthogonal base system for the S_{Pw} space

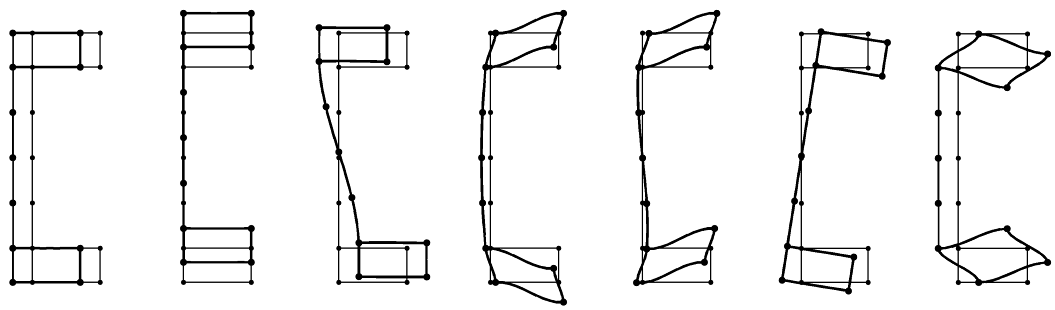

S_{Bt1} S_{Bt2} S_{Dt1} S_{Dt2} S_{Dt3} S_{Tt} S_{Ct1}

Figure A8: Cross-section orthogonal base system for the S_t space

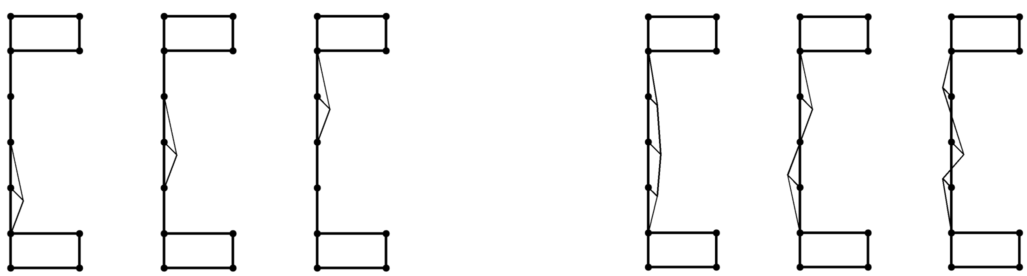

S_{S1} S_{S2} S_{S3} S_{S1} S_{S2} S_{S3}

Figure A9: Native (left) and cross-section orthogonal (right) base system for the S_S space

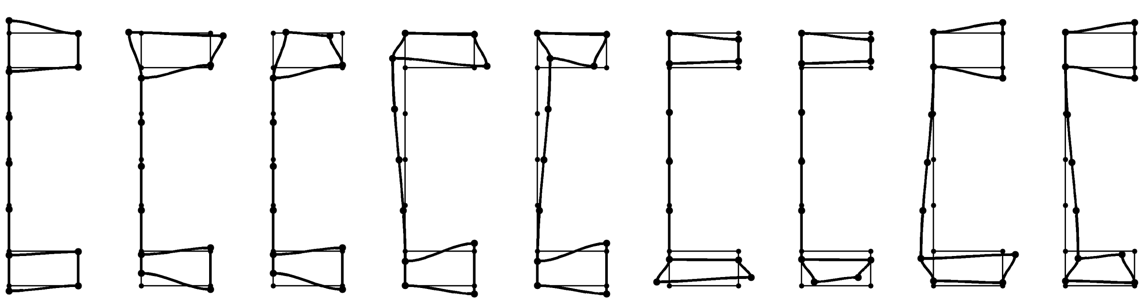

T_{P1} T_{P2} T_{P3} T_{P4} T_{P5} T_{P6} T_{P7} T_{P8} T_{P9}

Figure A10: Native base system for the T_P space

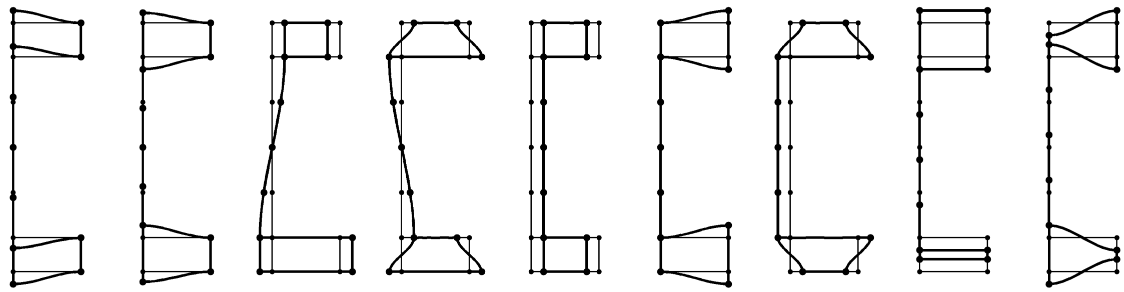

T_{P1} T_{P2} T_{P3} T_{P4} T_{P5} T_{P6} T_{P7} T_{P8} T_{P9}

Figure A11: Cross-section orthogonal base system for the T_P space

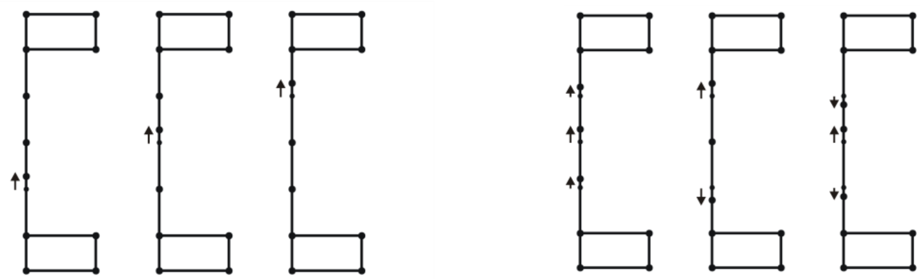

T_{S1} T_{S2} T_{S3} T_{S1} T_{S2} T_{S3}

Figure A12: Native (left) and cross-section orthogonal (right) base system for the T_S space